Published in final edited form as:
Cancer Cell. 2010 January 19; 17(1): 41–52. doi:10.1016/j.ccr.2009.11.023.

SIRT3 is a Mitochondrial Localized Tumor Suppressor Required for Maintenance of Mitochondrial Integrity and Metabolism During Stress

Hyun-Seok Kim[1,2], **Krish Patel**[1,3], **Kristi Muldoon-Jacobs**[3], **Kheem S. Bisht**[3], **Nukhet Aykin-Burns**[4], **J. Daniel Pennington**[3], **Riet van der Meer**[5], **Phuongmai Nguyen**[3], **Jason Savage**[3], **Kjerstin M. Owens**[6], **Athanassios Vassilopoulos**[2], **Ozkan Ozden**[3], **Seong-Hoon Park**[3], **Keshav K. Singh**[6], **Sarki A. Abdulkadir**[5], **Douglas R. Spitz**[4], **Chu-Xia Deng**[2,7], and **David Gius**[3,7]

[2]Genetics of Development and Disease Branch, NIDDK, NIH, Bethesda, MD 20892, USA

[3]Molecular Radiation Oncology, Radiation Oncology Branch, Center for Cancer Research, NCI, NIH, Bethesda, MD 20892, USA

[4]Free Radical and Radiation Biology Program, Department of Radiation Oncology, University of Iowa, Iowa City, IA 52242, USA

[5]Department of Pathology, Vanderbilt University Medical Center, Nashville, TN 37232, USA

[6]Department of Cancer Genetics, Roswell Park Cancer Institute, Buffalo, NY 14263, USA

SUMMARY

The sirtuin gene family (*SIRT*) is hypothesized to regulate the aging process and play a role in cellular repair. This work demonstrates that SIRT3$^{-/-}$ mouse embryonic fibroblasts (MEFs) exhibit abnormal mitochondrial physiology as well as increases in stress-induced superoxide levels and genomic instability. Expression of a single oncogene (*Myc* or *Ras*) in SIRT3$^{-/-}$ MEFs results in *in vitro* transformation and altered intracellular metabolism. Superoxide dismutase prevents transformation by a single oncogene in SIRT3$^{-/-}$ MEFs and reverses the tumor permissive phenotype as well as stress-induced genomic instability. In addition, SIRT3$^{-/-}$ mice develop ER/PR-positive mammary tumors. Finally, human breast and other human cancer specimens exhibit reduced *SIRT3* levels. These results identify *SIRT3* as a genomically expressed, mitochondrial localized tumor suppressor.

Keywords

SIRT3; Mitochondria; Carcinogenesis; Tumor suppressor

[7]Co-corresponding authors: David Gius, M.D., Ph.D., Chief, Molecular Radiation Oncology, National Cancer Institute, National Institutes of Health, 9000 Rockville Pike, Bethesda, MD 20892, Tel: (301) 435-9411, giusd@mail.nih.gov, Chu-Xia Deng, Ph.D., Section Chief, Genetics of Development and Disease Branch, NIDDK, National Institutes of Health, Bethesda, MD 20892, Tel: (301) 402-7225, chuxiad@mail.nih.gov.
[1]The first two authors contributed equally to this manuscript.

INTRODUCTION

An emerging theme in aging research is that sirtuin genes appear to regulate longevity in a wide variety of living systems from yeast to mammals (Sinclair, 2005; Tissenbaum and Guarente, 2001). Sirtuin genes are the human and murine homologs of the *Saccharomyces cerevisiae* Sir2 gene, which has been shown to regulate both replicative and overall lifespan (Guarente and Kenyon, 2000). The sirtuin genes are also central to the regulation of longevity in *C. elegans* and *D. melanogaster* (Rogina and Helfand, 2004). The mammalian sirtuin family consists of seven NAD+-dependent protein deacetylases that are localized to the nucleus (*SIRT1, 6*, and *7*), mitochondria (*SIRT3, 4*, and *5*), and cytoplasm (*SIRT2*), respectively, and that regulate a wide range of intracellular process (Haigis and Guarente, 2006).

The incidence of human malignancies increases exponentially as a function of aging, suggesting a mechanistic connection between aging (longevity) and carcinogenesis (Finkel et al., 2009). Mammalian cells contain fidelity proteins or tumor suppressor (TS) genes, such as p53, and loss of function of these proteins results in a damage permissive cell phenotype (Sherr, 2004). As such, the loss of function of these fidelity proteins is considered an early event in carcinogenesis. Since cancer is a disease of aging, and sirtuin genes appear to play a role in repair of cellular damage during aging, it is reasonable to propose that sirtuin genes may also have an anti-carcinogenic role and function as TSs (Saunders and Verdin, 2007; Wang et al., 2008). If so, it follows that loss of function of sirtuin genes may contribute to a tumor permissive phenotype (Deng, 2009).

It has also been suggested that the mitochondria play a central role in aging and carcinogenesis by generating reactive oxygen species as a byproduct of respiration (Singh, 2006). Mitochondrial abnormalities associated with altered oxidative metabolism are observed in tumor cells *in vitro* and *in vivo* and appear to contribute to a chronic condition of oxidative stress (Hsu and Sabatini, 2008). SIRT3 is one of the three genomically expressed sirtuins that localize to mitochondria (Onyango et al., 2002; Schwer et al., 2002) as well as the primary mitochondrial protein deacetylase (Lombard et al., 2007). In this regard, it is proposed that SIRT3 is ideally situated to function as a mitochondrial fidelity protein, and by extension, loss of function could result in a damage permissive and tumorigenic cellular environment.

RESULTS

SIRT3 knockout MEFs exhibit increased superoxide levels and chromosomal instability in response to exogenous stress

We have previously shown that HCT116 cells genetically altered to express a deacetylation-null mutant *SIRT3* gene ($SIRT3^{dn}$) have difficulty responding to increased reactive oxygen species (Jacobs et al., 2008). In addition, it has previously been shown that $SIRT3^{-/-}$ livers and MEFs have decreased total ATP levels and mitochondrial respiration (Ahn et al., 2008). As such, steady-state levels of superoxide were determined in $SIRT3^{+/+}$ and $SIRT3^{-/-}$ MEFs by following the oxidation of dihydroethidium (DHE) as mean fluorescence intensity (MFI). No differences in total cellular DHE oxidation levels were seen between the wild-type and *SIRT3* knockout MEFs that are cultured in 6% oxygen for these studies unless otherwise stated (Fig. 1A). However, in MEFs from a transgenic mouse expressing $SIRT3^{dn}$, a roughly two-fold increase in superoxide levels was observed (Supplemental section, Fig. S1A).

In contrast, a difference was observed in cells treated with two stress-inducing exogenous agents. Ionizing radiation (IR) and antimycin A, a mitochondrial electron transport chain (Complex III) inhibitor, represent genotoxic and metabolic stresses, respectively, that have

been hypothesized to cause an increase in mitochondrial superoxide levels (Aykin-Burns et al., 2009). Exposure of $SIRT3^{-/-}$ MEFs to either IR or antimycin A significantly increased intracellular superoxide levels, while only a comparatively modest increase was observed in $SIRT3^{+/+}$ cells (Fig. 1A). In addition, $SIRT3^{-/-}$ MEFs exhibited significantly higher intracellular superoxide levels when cultured at 21% O_2 for 6 hours (Fig. 1B), compared to either $SIRT3^{+/+}$ or $SIRT3^{-/-}$ MEFs that are routinely grown at 6% O_2 or $SIRT3^{+/+}$ MEFs cultured at 21% O_2.

Mitochondrial superoxide levels (measured using Mito-SOX oxidation) were elevated in the $SIRT3^{-/-}$ MEFs and significantly increased following exposure to either IR or antimycin A (Fig. 1C). In contrast, a much smaller increase in mitochondrial superoxide levels was observed in irradiated or antimycin A treated $SIRT3^{+/+}$ MEFs. An increase in mitochondrial superoxide level was also observed in the $SIRT3^{-/-}$ MEFs at 21% O_2 (Supplemental Fig. S1B). These results suggest that loss of *SIRT3* may allow exogenous stressing agents to more readily disrupt oxidative metabolism, leading to increased steady-state levels of superoxide.

Cellular exposure to exogenous genotoxic stress, such as IR, has previously been shown to induce chromosomal aberrations, and one mechanism accounting for this observation has been hypothesized to involve increased intracellular superoxide levels (Spitz et al., 2004). Chromosome analysis of at least 100 metaphases from $SIRT3^{+/+}$ or $SIRT3^{-/-}$ MEFs showed a chromosome complement of 40 ± 2 in both knockout and wild-type cells. In contrast, a relatively modest dose of radiation (2 and 5 Gy) caused a significant increase in chromosome number in the $SIRT3^{-/-}$ MEFs after 72 hrs (Fig. 1D), suggesting that loss of *SIRT3* results in chromosomal instability induced by genotoxic stress.

SIRT3 knockout livers and MEFs have decreased mitochondrial integrity with age

It has previously been suggested that nuclear sirtuins may function as fidelity proteins that play a role in the maintenance of genomic integrity (Wang et al., 2008). Since SIRT3 is localized to the mitochondria (Onyango et al., 2002; Schwer et al., 2002), it seemed logical to investigate if it might also play a role in the maintenance of mitochondrial DNA (mtDNA) integrity. Livers from *SIRT3* knockout mice at 20, 36, and 58 weeks showed a gradual decrease in mtDNA integrity, as measured by the amplification efficiency for a large (10,095 bp) fragment of mtDNA, compared to isogenic wild-type mice (Fig. 1E). *SIRT3* knockout MEFs also showed a decrease in mtDNA integrity that was first observed at passage number 6 (Fig. 1F) and was further decreased at passage number 10, as compared to $SIRT3^{+/+}$ MEFs. The amplification efficiency of a small control 117-bp fragment was unchanged in both the livers (Supplemental Fig. S1C) and MEFs (Fig. S1D).

SIRT3 knockout MEFs do not spontaneously immortalize

It is well established that mitochondrial abnormalities, including those associated with altered mitochondrial metabolism, are observed in tumor cells *in vitro* and in human malignancies (Singh, 2006; Warburg, 1956). We therefore determined if *SIRT3* knockout MEFs would exhibit altered growth characteristics as compared to $SIRT3^{+/+}$ MEFs. $SIRT3^{+/+}$ and $SIRT3^{-/-}$ MEFs at passage 3 were cultured identically and at passage 8 exhibited increased doubling times, and neither was able to divide beyond cell passage 15 (data not shown). These primary cells have identical doubling times (data not shown). Thus, $SIRT3^{+/+}$ and $SIRT3^{-/-}$ MEFs do not have the ability to divide beyond passage 15 and as such, cannot spontaneously immortalize (see methods for further description).

These MEFs at passage three were also measured for loss of contact inhibited cell growth via colony formation assays. This assay measures the ability of tissue culture cells plated to

confluence to spontaneously form colonies, which are defined as concentrated nests of cells that pile up and grow on top of each other. MEFs were plated at 10^6 in a 100 mm dish and the medium was changed every two days until 28 days, when cells were stained with crystal violet. SIRT3$^{-/-}$ MEFs stained after 28 days formed a greater number of colonies (Fig. 2A and 2B, bars 1–2), relative to SIRT3$^{+/+}$ MEFs. In addition, SIRT3$^{-/-}$ MEFs exhibited decreased stress-induced apoptosis in response to either IR (2 and 5 Gy) or camptothecin (Supplemental Fig. S2A) and these results are in agreement with previously published results (Allison and Milner, 2007) suggesting SIRT3 is a general pro-apoptotic factor. These results suggest that SIRT3$^{-/-}$ MEFs have decreased stress-induced apoptosis as well as relatively low frequency of contact inhibition; however, these cells cannot grow beyond passage 15, and therefore did not spontaneously immortalize.

SIRT3$^{-/-}$ MEFs expressing a single oncogene display a transformation-permissive phenotype

It was shown over twenty years ago that primary immortalized cells can be transformed *in vitro* by the cooperation of at least two oncogenes, such as *Ras* and *Myc* (Land et al., 1986; Parada et al., 1984), validating the Knudson two-hit model for carcinogenesis (Knudson, 1971). This idea has been extended to show that inactivation or deletion of a TS gene can complement the activation of a single oncogene, resulting in cellular transformation (Sherr, 2004).

To determine if loss of *SIRT3* results in an *in vitro* transformation-permissive phenotype, SIRT3$^{+/+}$ and SIRT3$^{-/-}$ MEFs were infected with lentivirus expressing either *Myc* or *Ras*. It has been previously shown that overexpression of *Myc* in primary cells results in massive programmed cell death, while overexpression of *Ras* induces premature senescence (Sebastian et al., 2005; Serrano et al., 1997). Consistent with previous findings, SIRT3$^{+/+}$ MEFs exhibited *in vivo* immortalization (see methods for description) after infection with both *Myc* and *Ras*, but not with either *Myc* or *Ras* alone (Table 1). In contrast, SIRT3$^{-/-}$ MEFs infected with either *Myc* or *Ras* alone became immortalized, as well as cells infected with both genes (Table 1). In addition, MEFs from a transgenic mouse expressing SIRT3^{dn} (amino acid 248 changed from histidine to tyrosine) and lacking SIRT3 (SIRT3^{dn}-SIRT3$^{-/-}$) were also immortalized by a single oncogene. In contrast, SIRT3^{wt}-SIRT3$^{-/-}$ MEFs required both *Myc* and *Ras* (Table 1). PCR and western analysis confirmed viral integration and expression of *Myc* and *Ras* (data not shown). These results suggest that *SIRT3* may act as a TS by substituting for one of the two oncogenes required for *in vitro* immortalization (see methods for description).

SIRT3$^{+/+}$, SIRT3$^{+/+}$ Myc/Ras, SIRT3$^{-/-}$, SIRT3$^{-/-}$ Myc, SIRT3$^{-/-}$ Ras, and SIRT3$^{-/-}$ Myc/Ras (referred to hereafter as 'the panel') MEFs were plated at 1×10^6/100 mm dish for a total of 28 days and contact inhibited cell growth was determined. SIRT3$^{-/-}$ Ras and SIRT3$^{-/-}$ Myc/Ras cells displayed a sizeable increase in focal colony formation (Fig. 2B, bars 4 and 6), while SIRT3$^{-/-}$ Myc and SIRT3$^{+/+}$ Myc/Ras (bars 3 and 5) showed a slight increase, as compared to SIRT3$^{+/+}$ and SIRT3$^{-/-}$ MEFs (bars 1 and 2). These results reveal that cells lacking *SIRT3* display a significant loss of contact inhibition in response to oncogene expression.

Another cell biological criterion of *in vitro* transformation is the ability of cells to form colonies when plated at very low cell densities, which is a measure of increased mitotic activity or reproductive integrity. As such, the panel of MEFs was plated at either 100 or 250 cells per well in 60 mm 6-well tissue culture plates and stained with crystal violet after 10 days (Fig. 2C). The results of these experiments show that cells lacking *SIRT3* and expressing *Myc*, *Ras*, or *Myc*/*Ras* form more colonies than *SIRT3* wild-type cells expressing both *Myc* and *Ras*. The transformed SIRT3$^{-/-}$ Myc, SIRT3$^{-/-}$ Ras, and SIRT3$^{-/-}$

Myc/Ras cells also exhibit less basal apoptosis than the SIRT3$^{+/+}$ Myc/Ras cells (Supplemental Fig. S2B). Finally, SIRT3$^{-/-}$ Myc/Ras, SIRT3$^{-/-}$ Ras, and SIRT3$^{-/-}$ Myc cells exhibited a more transformed morphology as shown by random cell orientation, changes in cellular architecture, and nuclear to cytoplasmic ratios (data not shown).

Loss of SIRT3 results in an invasive and tumorigenic phenotype

The frequency of aneuploidy and/or polyploidy has been suggested as one of many biomarkers that may be proportional to the degree of malignancy of a tumor (Deng, 2006). Fluorescence-activated cell sorting (FACS) analysis demonstrated that SIRT3$^{-/-}$ Myc, SIRT3$^{-/-}$ Ras, and SIRT3$^{-/-}$ Myc/Ras cells have significantly more polyploid cells (Fig. 3A) and chromosomal analysis showed more aneuploidy (Fig. 3B) than measured in the SIRT3$^{+/+}$, SIRT3$^{+/+}$ Myc/Ras, or SIRT3$^{-/-}$ cell lines. The results of these cell biological experiments suggest that cells lacking *SIRT3* and overexpressing at least one exogenous oncogene exhibit a more *in vitro* transformed phenotype than wild-type *SIRT3* cells expressing two oncogenes (*Myc* and *Ras*).

Cell growth in soft agar and athymic nude mice are well-established systems in which to assess anchorage independent growth and tumorigenesis, respectively. It has been demonstrated that MEFs immortalized with two oncogenes, such as *Myc* and *Ras*, have altered growth properties but do not grow in soft agar or form allograft tumors in nude mice unless an additional genetic event occurs (Land et al., 1986). Anchorage independent growth was determined by examining cell growth in soft agar, and these experiments showed that SIRT3$^{-/-}$ Ras, SIRT3$^{-/-}$ Myc/Ras, and, to a smaller degree, SIRT3$^{-/-}$ Myc cells have an anchorage independent phenotype (Fig. 3C). To determine *in vivo* tumorigenesis, 10^6 cells were implanted into the hind limbs of nude mice. After three weeks, the SIRT3$^{-/-}$ Myc/Ras cell lines were able to grow (in 6/6 mice) allograft tumors (Fig. 3D) consistent with a poorly differentiated sarcoma (Fig. 3E), while no tumors were observed for either the SIRT3$^{+/+}$ Myc/Ras or the other cell lines (0/6 mice). These results suggest that loss of *SIRT3*, when combined with *Myc* and *Ras*, provides a necessary genetic event resulting in tumorigenesis.

SIRT3 knockout transformed MEFs display altered intracellular metabolism

We have shown that *SIRT3* knockout MEFs demonstrate normal steady-state levels of superoxide under unstressed conditions, but exhibit a stress-induced increase in superoxide levels. As such, superoxide levels were measured in transformed *SIRT3* knockout cells to determine whether the genetic loss of *SIRT3* combined with oncogene transformation created an increased prooxidant intracellular environment. SIRT3$^{-/-}$ Ras, SIRT3$^{-/-}$ Myc/Ras, and, to a lesser extent, SIRT3$^{-/-}$ Myc cells exhibited higher steady-state levels of total cellular superoxide (Fig. 4A) as well as mitochondrial superoxide levels (Supplemental Fig. S3A).

The SIRT3$^{-/-}$ Ras and SIRT3$^{-/-}$ Myc/Ras cells exhibit increased total cellular ATP levels (Fig. 4B) when compared to the SIRT3$^{+/+}$ Myc/Ras or untransformed SIRT3$^{+/+}$ MEFs (data not shown). Surprisingly, the SIRT3$^{-/-}$ Ras and SIRT3$^{-/-}$ Myc/Ras cells had significantly decreased mitochondrial ATP levels (Fig. 4C, Supplemental Fig. S3B). These results suggest that the transformed *SIRT3* knockout cells are more metabolically active but are generating this energy from sources other than mitochondrial oxidative phosphorylation, and are either producing more reactive oxygen species or have a decreased ability to scavenge superoxide.

SIRT3 knockout transformed MEFs display increased glycolysis and decreased oxidative phosphorylation

It is well established that tumor cells consume glucose at a much greater rate than nontransformed cells, and this is referred to as the Warburg effect (Warburg, 1956). As such, glucose metabolism was monitored in the panel of MEF cell lines. Figure 4D shows that *SIRT3* knockout cells infected with *Myc*, *Ras*, or *Myc* and *Ras* consume increased amounts of glucose.

One potential mechanism accounting for the observed increases in intracellular superoxide and glycolysis in the SIRT3$^{-/-}$ Ras and SIRT3$^{-/-}$ Myc/Ras cells might involve changes in the level of oxidative phosphorylation. As such, the activities of electron transport complexes I, II, III and IV were determined in the *SIRT3* wild-type and knockout transformed cell lines. These experiments showed a significant decrease in complex I and complex III activity in the SIRT3$^{-/-}$ Ras and SIRT3$^{-/-}$ Myc/Ras cells, as compared to the SIRT3$^{+/+}$ Myc/Ras cells (Fig. 4E). These results confirm that loss of *SIRT3* alters complex I activity (Ahn et al., 2008) (Supplemental Fig. S3C) and suggest a role for SIRT3 in the regulation of complex III. This also suggests that the SIRT3$^{-/-}$ Myc/Ras and SIRT3$^{-/-}$ Ras cells have a decreased ability to generate sufficient ATP by oxidative phosphorylation to keep up with the increased demands of proliferation. This is consistent with the decrease in mtATP levels observed in the SIRT3$^{-/-}$ Ras and SIRT3$^{-/-}$ Myc/Ras cells (Fig. 4C). Therefore, these cells may enhance metabolism of glucose in glycolysis to increase the production of ATP. Alternatively, glucose metabolism could also be increased to generate reducing equivalents to detoxify hydroperoxides formed from higher steady-state levels of superoxide and hydrogen peroxide (Aykin-Burns et al., 2009). In addition, the decreased activities of complexes I and III could increase the residence times of electrons at sites where univalent reduction of O_2 to form superoxide could occur (Spitz et al., 2004).

SOD decreases SIRT3$^{-/-}$ Ras- and Myc/Ras-induced growth properties and prevents transformation of SIRT3$^{-/-}$ MEFs by a single oncogene

SIRT3$^{-/-}$ Ras and SIRT3$^{-/-}$ Myc/Ras cells formed larger colonies when plated at low densities (Fig. 2C), suggesting that these cells have increased growth rates. These results were confirmed by cell growth assays demonstrating that *SIRT3* knockout cells expressing *Myc* and/or *Ras* proliferate faster than wild-type cells. These cells fell into two distinct groups: SIRT3$^{-/-}$ Ras and SIRT3$^{-/-}$ Myc/Ras cells had shorter doubling times than SIRT3$^{-/-}$ Myc and SIRT3$^{+/+}$ Myc/Ras cells (Fig. 5A). To investigate the idea that increased reactive oxygen species, and specifically superoxide, may be pro-proliferative in *SIRT3* knockout transformed cells, an adenoviral vector that causes enforced overexpression of manganese superoxide dismutase was utilized (AdMnSOD) (Aykin-Burns et al., 2009). AdMnSOD, which decreases steady-state levels of superoxide (Supplemental Fig. S4A), was used to overexpress *MnSOD* in transformed *SIRT3* knockout cells. AdMnSOD increased the cell doubling time of the SIRT3$^{-/-}$ Ras and SIRT3$^{-/-}$ Myc/Ras but not the SIRT3$^{+/+}$ Myc/Ras cells (Fig. 5B), suggesting that excess superoxide favors increased cell proliferation.

To determine if increased mitochondrial superoxide was required for the immortalization of SIRT3$^{-/-}$ MEFs, *Myc* and *Ras* infections were repeated in the presence a lentivirus expressing *MnSOD* (lenti-MnSOD, a kind gift from Dr. Rezvani, Columbia University). Infection of lenti-MnSOD 24 hours prior to exposure to IR prevented the increase in IR-induced mitochondrial superoxide levels (Supplemental Fig. S4B) that was observed in the SIRT3$^{-/-}$ MEFs (Fig. 1C). While immortalization of SIRT3$^{-/-}$ cells infected with both *Myc* and *Ras* was not affected, coinfection with lenti-MnSOD prevented immortalization of SIRT3$^{-/-}$ cells infected with only one oncogene (Table 1). Expression of the lentiviral

exogenous MnSOD was confirmed (data not shown). The results of these experiments suggest that elevated superoxide levels in *SIRT3* knockout cells play a central role in immortalization.

We have shown earlier that SIRT3$^{-/-}$ cells have increased stress-induced superoxide levels (Fig. 1A–B), including when these MEFs routinely cultured at 6% O_2 were subsequently grown at 21% O_2 (Fig. 1B), suggesting that superoxide may be at least one mechanism promoting cellular transformation (Table 1). Thus, it seemed reasonable to determine if long term growth at 21% O_2 will increase the loss of contact inhibition phenotype as determined by colony formation assays (Fig. 2A–B). As such, SIRT3$^{+/+}$ and SIRT3$^{-/-}$ MEFs were cultured at 21% O_2 for 28 days to determine if these conditions would increase cell contact inhibition. A roughly five-fold increase in loss of contact inhibition, as determined by colony formation, was observed in the SIRT3$^{-/-}$ MEFs grown at 21% (Fig. 5C, bar 2 versus 4), while no difference was observed in the SIRT3$^{+/+}$ MEFs (bar 1 versus 3). Similar to the results observed in Table 1, the addition of lenti-MnSOD reversed the increase in colonies formed when SIRT3$^{-/-}$ cells were grown at 21% O_2 for 28 days (Fig. 5D, bar 2 versus 4,) as well as the overall density of the colonies (data not shown). Finally, we previously showed that SIRT3$^{-/-}$ MEFs exposed to IR displayed an increase in total cellular superoxide levels (Fig. 1A) and genomic instability (Fig. 1D). When these experiments were repeated in the presence of MnSOD (Fig. 5E), the IR-induced increase in aneuploidy was prevented.

These results suggest that the increase in superoxide observed in the SIRT3$^{-/-}$ MEFs plays a role, at least in part, in the tumor-permissive phenotype. To address this idea, *MnSOD* expression was determined in wild-type and *SIRT3* knockout mouse livers at 5, 9, and 13 months. A slight decrease in *MnSOD* expression was observed at 9 months that became statistically significant at 13 months (Fig. 5F, Supplemental Fig. S4C). In contrast, no significant change in *MnSOD* expression was observed in the wild-type mice. A decrease in *MnSOD* expression was also observed in the transformed SIRT3$^{-/-}$ Ras and SIRT3$^{-/-}$ Myc/Ras cells (Supplemental Fig. S4D), which have previously been shown to have increased superoxide levels compared to the SIRT3$^{+/+}$ Myc/Ras cells (Fig. 4A). Finally, similar to the SIRT3$^{-/-}$ MEFs, MnSOD$^{-/-}$ MEFs (a kind gift from Prabhat Goswami, University of Iowa) are also immortalized by a single oncogene (Supplement, Table S1) suggesting that loss of *MnSOD* may also result in an immortalization permissive phenotype.

ChIP analysis of SIRT3$^{+/+}$ and SIRT3$^{-/-}$ livers showed decreased binding of two primary transcription factors that regulate *MnSOD*, FOXO3a and NF-κB (Supplemental Fig. S4E), to the MnSOD promoter at 13 months but not 5 months (data not shown). No change in total (Supplemental Fig. S4F) or mitochondrial (data not shown) FOXO3a or NF-κB was observed in SIRT3$^{+/+}$ or SIRT3$^{-/-}$ age-matched mice. However, SIRT3 deacetylates FOXO3a (Supplemental Fig. S4G) and there is a significant increase in phospho-FOXO3a levels in cells expressing SIRT3^{dn}, as compared to cells expressing the wild-type *SIRT3* (Supplemental Fig. S4H, lower panel). These results are consistent with recently published data (Sundaresan et al., 2009). Finally, cells expressing SIRT3^{dn} contain decreased nuclear FOXO3a protein levels (Supplemental Fig. S4I), as shown by others (Sundaresan et al., 2009). These results suggest that loss of SIRT3 deacetylation activity decreases FOXO3a nuclear localization.

Finally, transfection with a vector expressing a constitutively active *FOXO3a* dominant positive gene (pCMV-N-FOXO3a), which increases nuclear FOXO3a protein levels (Jacobs et al., 2008), prevented immortalization of SIRT3$^{-/-}$ MEFs by a single (Myc or Ras) oncogene (Supplement, Table S1). These results suggest that nuclear import of FOXO3a may play a role, at least in part, in an immortalization permissive phenotype.

SIRT3 wild-type, but not a deacetylation null mutant gene, induces MnSOD gene expression and decreases mitochondrial superoxide levels

MnSOD protein levels are decreased in the $SIRT3^{-/-}$ Myc/Ras (Fig. 5G, bar 1), as compared to the $SIRT3^{+/+}$ Myc/Ras (bar 2) cells. As such, $SIRT3^{-/-}$ Myc/Ras cells were infected with lentivirus expressing either a wild-type *SIRT3* (lenti-SIRT3-wt) or a deacetylation null mutant *SIRT3* (Ahn et al., 2008) gene (lenti-SIRT3-dn). These experiments showed that the wild-type (Fig. 5G, bar 1 versus 3), but not the deacetylation null mutant SIRT3 (bar 4) gene, increased MnSOD protein levels to those observed in the wild-type $SIRT3^{+/+}$ Myc/Ras MEFs (bar 2). Exogenous Myc tagged SIRT3 expression was confirmed by western blotting (data not shown). In addition, lenti-SIRT3-wt, but not lenti-SIRT3-dn, reversed the increase in mitochondrial superoxide levels observed in the $SIRT3^{-/-}$ Myc/Ras cells (Fig. 5H). Finally, $SIRT3^{+/+}$ Myc/Ras MEFs cells infected with retroviruses expressing two different *SIRT3* shRNAs also decreased *MnSOD* expression (Supplemental Fig. S4J). These results suggest a more direct link between SIRT3 deacetylation and *MnSOD* expression as well as altered mitochondrial metabolism.

SIRT3 is a mitochondrial localized murine tumor suppressor

SIRT3 knockout MEFs are immortalized and transformed *in vitro* by the expression of a single oncogene, suggesting that loss of *SIRT3* results in a tumor-permissive phenotype. Thus, we investigated whether *SIRT3* knockout mice developed tumors. $SIRT3^{-/-}$ mice were healthy, and no outwardly observed phenotype was noted (Lombard et al., 2007); however, seven of twenty female mice developed mammary gland tumors (Fig. 6A) over 24 months (Fig. 6B), while zero $SIRT3^{+/+}$ mice developed mammary tumors during the same period. Histological H&E examination of these mammary tumors showed a characteristic invasive ductal carcinoma (Fig. 6C). In addition, single, but not double, positive immunohistochemistry (IHC) staining, was observed for cytokeratin 14 (CK14), a basal epithelial cell marker, or CK18, a luminal epithelial cell marker (Fig. 6D), suggesting a well differentiated histological pathology. IHC identified these tumors as estrogen receptor and progesterone receptor (ER/PR)-positive (Fig. 6E). These results parallel a well differentiated, receptor-positive histological characteristic that is commonly observed in breast malignancies in older women.

$SIRT3^{-/-}$ mouse livers exhibit increased mtDNA damage and decreased *MnSOD* expression with age and develop mammary tumors after 12 months, suggesting that cellular reactive oxygen species might increase with age in the $SIRT3^{-/-}$ mice. Mammary tissue isolated from $SIRT3^{+/+}$ and $SIRT3^{-/-}$ mice were stained with an anti-nitrotyrosine antibody as a marker for increased protein damage caused by intracellular reactive oxygen/nitrogen species, since increased nitrotyrosine formation on proteins is believed to reflect increased formation of $ONOO^{-}$, which is the reaction product of nitric oxide and superoxide. *SIRT3* knockout mouse mammary ductal cells exhibited increased anti-nitrotyrosine staining (StressMarq Biosciences Inc.) at 12 months (Fig. 6F, Supplemental Fig. S5), while no differences were detected at 5 months (data not shown). This suggests that increased oxidative/nitrosative damage to proteins is occurring in the mammary tissues of $SIRT3^{-/-}$ animals as a function of age.

SIRT3 is a potential human tumor suppressor

The hypothesis that *SIRT3* may serve as a tumor suppressor *in vivo* was further supported by the observation that *SIRT3* expression is decreased in breast cancer specimens from a commercially available tissue array (US Biomax, Inc.), as compared to normal breast tissue samples (Fig. 7A). In addition, zero of nine metastatic lymph nodes positively stained for SIRT3 (data not shown). IHC staining also confirmed that SIRT3 localizes to normal

mammary ductal cells (Fig. 7B). *SIRT3* RNA expression is also decreased in Stage IIA, IIB, and III malignancy breast samples (TissueScan Breast Cancer Panel 1, Origene) (Fig. 7C).

The Oncomine cancer microarray database (Rhodes et al., 2007) was subsequently used to determine if *SIRT3* expression is decreased in human malignancies. *SIRT3* was decreased in breast tumors as compared to normal breast (Fig. 7D) and as a function of both Elston Grade (G-1, G-2, or G-3) (Fig. 7E, Supplemental Fig. S6A) and pathological differentiation (well, moderately, or poorly differentiated) (Fig. 7F, Supplemental Fig. S6B). Finally, *SIRT3* expression was also decreased in several other human malignancies including testicular (Supplement Figs. S6C), glioblastoma multiforme (Fig. S6D), prostate (Figs. S6E), head and neck squamous cell (Fig. S6F), clear cell renal (Fig. S6G), and hepatocellular (Fig. S6H) cancers.

DISCUSSION

While there is no universal definition of a TS gene, for the purposes of this work, we defined a TS gene as one that: (1) protects a tissue culture cell from one step on the path to *in vitro* transformation; (2) results in tumorigenesis in murine models lacking expression; (3) is decreased in human malignancies; and (4) results in the loss of functional organelle integrity or the accumulation of cellular damage to critical biomolecules either spontaneously or following exposure to stress. Based on these criteria we propose that SIRT3 is a mitochondrial TS.

In this regard, we demonstrated that SIRT3$^{-/-}$ MEFs infected with a single oncogene become immortalized as well as *in vitro* transformed, and that they exhibit anchorage independent growth. Furthermore, SIRT3$^{-/-}$ MEFs expressing *Myc* and *Ras* grew in nude mice, suggesting that loss of *SIRT3* also results in an *in vivo* tumorigenic phenotype. In addition, *SIRT3* knockout mice spontaneously form mammary tumors later in life. Finally, *SIRT3* protein levels are decreased in human breast cancers as well as several other human malignancies. In our murine model SIRT3 appears to be limited to the mitochondria. Thus, we propose that SIRT3 is a genomically expressed, mitochondrially localized TS.

Interestingly, the murine mammary tumors we assayed were well differentiated, ER/PR-positive. In humans, these markers are most often seen in tumors from women who develop breast cancer later in life. Since sirtuins are the human homologs of longevity genes in *C. elegans* and yeast (Tissenbaum and Guarente, 2001), this result suggests that the *SIRT3* knockout mouse may be useful as a model for an ER/PR-positive subtype of breast cancer that is more commonly observed in women over 65 years of age.

In this work we have also shown that the transformed SIRT3$^{-/-}$ Myc/Ras cells, but not the wild-type Myc/Ras cells, have significant increases in glucose metabolism, superoxide levels, and total cellular ATP levels, but decreased ATP from oxidative phosphorylation. However, it is unclear if this was due to loss of *SIRT3* or the natural process of transformation. In addition, the activity of complexes I and III of the electron transport chain was significantly decreased in the SIRT3$^{-/-}$ Myc/Ras and SIRT3$^{-/-}$ Ras cells, as compared to SIRT3$^{+/+}$ Myc/Ras cells. This could explain why the addition of lentivirus MnSOD prevented the immortalization of SIRT3$^{-/-}$ cells by *Myc* or *Ras* alone; however, expression of both *Myc* and *Ras* provided an additional pro-proliferation event that pushed the cells over the edge toward immortalization, transformation, and tumorigenesis. Finally, the i*n vivo* situation might be more complex than in cultured cell model as that data showed that the decreased *MnSOD* expression was only observed in older *SIRT3* mutant mice. This issue is potentially interesting and will be investigated in future studies.

Eukaryotic cells contain fidelity proteins that function to monitor the integrity of critical intracellular processes, and deletion or mutation of the corresponding genes results in a cellular environment permissive for the accumulation of DNA damage (Hunter, 1997). Thus, it seems like a logical extension that the mitochondria would also contain fidelity proteins to maintain the integrity of the mitochondria. In this regard, loss of *SIRT3* results in a decrease in *MnSOD* as a function of age resulting in an increase in mitochondrial superoxide and perhaps other ROS (Fig. 7G). This may create a cellular environment permissive for *in vivo* carcinogenesis including receptor positive mammary tumors that are observed in the *SIRT3* knockout mice after age 13 months. As such, we propose that *SIRT3* functions as a genomically expressed, mitochondrially localized fidelity protein, in addition to meeting the criteria to be classified as a TS.

Experimental Procedures

Cell lines

MEFs were isolated from E14.5 isogenic $SIRT3^{+/+}$ and $SIRT3^{+/+}$ mice and maintained in a 37 °C incubator with 5% CO_2 and 6% oxygen except when otherwise noted. $SIRT3^{+/+}$ or $SIRT3^{-/-}$ MEFs were infected at passage 3 with lentivirus expressing either *Myc, Ras* or *MnSOD* were made by Applied Biological Materials, Inc. (Richmond, British Columbia), and pooled selected cells were used for all experiments. For this study our definition of *spontaneous immortalization* of primary MEFs is the ability to continue dividing past passage 15 and subsequently divide indefinitely. For *in vitro immortalization* experiments via enforced genetic expression of one or two oncogenes, MEFs at passage 3 were infected with a lentivirus containing *Myc*, *Ras*, or both. Cells were cultured and split every two days to prevent confluency and plated into a new 100 mm dish at 3.0×10^5 cells. After 17 additional passages (20 total), cells were considered immortalized if they continued to divide.

MEFs were infected with 5 MOI of virus per 10 cm / plate. Levels of *Myc* and *Ras* were confirmed by western blot analysis, and PCR analysis (data not shown). Soft agar and colony formation assays were done as previously described (Supplemental Methods).

Statistical analysis

Data were analyzed by Student's t-test, and results were considered significant at $p<0.05$. Results are presented as mean ± S.D.

Measurement of intracellular superoxide levels

Superoxide production was determined as described (Slane et al., 2006) using the fluorescent dye dihydroethidium (DHE), obtained from Molecular Probes (Eugene, Oregon). Mitochondrial superoxide levels were determined by the addition of Mito-SOX (3 μM) to the cells, cultured as described above and incubated for an additional 10 minutes before being trypsinized and resuspended and measured by fluorescence (Molecular Probes). See supplemental section for detail.

Measurement of glucose consumption, ATP levels, and oxygen consumption

Glucose consumption per cell was measured by plating 300,000 cells on a 60-mm plate. Cells were given fresh medium at time zero. Cells were counted and medium samples were obtained at 48 hours and analyzed using a YSI glucometer. Glucose consumption was determined by subtracting glucose content at 48 hours from the time zero samples and dividing by the number of cells.

Total ATP levels were monitored using a CellTiter-Glo Luminescent Cell Viability Assay as per the manufacturer's instructions (Promega). CellTiter-Glo was added to 10^6 cells and placed on an orbital shaker to induce cell lysis, and samples were read on a chemiluminescence plate reader (Tecam Safire; integration time of 1 s). Mitochondrial ATP was determined by incubating MEFs in 20 mM 2DG and 5 mM pyruvate for 4 and 24 hours prior to using an adenosine 5'-triphosphate bioluminescent somatic cell assay kit (Supplemental methods).

Oxygen consumption was measured using the YSI oxygen monitor containing a Clarktype electrode as per the manufacturer's instructions. The cell pellet was resuspended at a density of 2.5×10^6 cells/mL in PBS containing 5 mM glucose. For each sample, a 3 mL sample was placed in the electrode chamber and allowed to equilibrate with air for 3 min. Oxygen consumption was then recorded for 15 min. The data were normalized to cell number.

Chromosome aberrations

MEFs were exposed at passage four to irradiation and harvested after 72 hours. Whole-mount chromosomes were counted in a blinded fashion. Individual spreads were deemed countable if all chromosomes were clearly defined and clearly visible within the ghost of a single cytoplasm.

Real-time long PCR assay for mtDNA damage

mtDNA damage was measured as amplification efficiency for a large (10,095 bp) fragment relative to a short (117 bp) Amplicon of mtDNA in wild-type and knockout mice (see Supplemental Methods).

Allograft and Tissue Specimen

Cells (2×10^6 or 1×10^6) in PBS for a total volume of 100 μL/injection site were injected subcutaneously in right and left flanks of 8-week-old male athymic mice (Jackson Laboratories).Tumor sizes were measured twice weekly in two dimensions (width, W and length, L) with calipers. Average tumor volume (V) was calculated as $V = 0.5 \times L \times W^2$. At the termination of the experiment, mice were sacrificed; tumors were excised and weighed. All animal care followed approved institutional guidelines of the NIH All experiments were approved by the animal care and use committee of the National Institute Diabetes and Digestive and Kidney Diseases (K069-GDDB-08) or the National Cancer Institute (ROB-118).

Normal and breast cancer tissue slides were purchased from (US Biomax, Inc) and analyzed by IHC. RNA samples from normal breast (NB) and malignant breast were purchased (TissueScan Breast Cancer Panel 1 Origene) and analyzed per the supplier's instructions. As these samples were obtained commercially without accompanying patient identifying data, they are considered "exempt" according to HHS guidelines.

Oxidative phosphorylation enzyme activities

Oxidative phosphorylation enzyme activities were measured on total cellular protein including complex I (Supplemental Methods). Complex II, III, and IV methods are presented in the supplemental section.

Supplementary Material

Refer to Web version on PubMed Central for supplementary material.

Acknowledgments

This research was supported (in part) by the Intramural Research Program of the NIDDK, NCI, and CCR, NIH. DRS and NAB are supported by grants from the National Institutes of Health (R01CA100045, R01CA133114, and P30 CA086862). KKS was supported by R01 121904 and 116430. We thank Melissa Stauffer, PhD, of Scientific Editing Solutions, for editorial assistance.

REFERENCES

Ahn BH, Kim HS, Song S, Lee IH, Liu J, Vassilopoulos A, Deng CX, Finkel T. A role for the mitochondrial deacetylase Sirt3 in regulating energy homeostasis. Proc Natl Acad Sci U S A. 2008; 105:14447–14452. [PubMed: 18794531]

Allison SJ, Milner J. SIRT3 is pro-apoptotic and participates in distinct basal apoptotic pathways. Cell cycle (Georgetown, Tex. 2007; 6:2669–2677.

Aykin-Burns N, Ahmad IM, Zhu Y, Oberley LW, Spitz DR. Increased levels of superoxide and H2O2 mediate the differential susceptibility of cancer cells versus normal cells to glucose deprivation. Biochem J. 2009; 418:29–37. [PubMed: 18937644]

Deng CX. BRCA1: cell cycle checkpoint, genetic instability, DNA damage response and cancer evolution. Nucleic acids research. 2006; 34:1416–1426. [PubMed: 16522651]

Deng CX. SIRT1, is it a tumor promoter or tumor suppressor? International journal of biological sciences. 2009; 5:147–152. [PubMed: 19173036]

Finkel T, Deng CX, Mostoslavsky R. Recent progress in the biology and physiology of sirtuins. Nature. 2009; 460:587–591. [PubMed: 19641587]

Guarente L, Kenyon C. Genetic pathways that regulate ageing in model organisms. Nature. 2000; 408:255–262. [PubMed: 11089983]

Haigis MC, Guarente LP. Mammalian sirtuins--emerging roles in physiology, aging, and calorie restriction. Genes Dev. 2006; 20:2913–2921. [PubMed: 17079682]

Hsu PP, Sabatini DM. Cancer cell metabolism: Warburg and beyond. Cell. 2008; 134:703–707. [PubMed: 18775299]

Hunter T. Oncoprotein networks. Cell. 1997; 88:333–346. [PubMed: 9039260]

Ivshina AV, George J, Senko O, Mow B, Putti TC, Smeds J, Lindahl T, Pawitan Y, Jacobs KM, Pennington JD, Bisht KS, Aykin-Burns N, Kim HS, Mishra M, Sun L, Nguyen P, Ahn BH, Leclerc J, et al. SIRT3 interacts with the daf-16 homolog FOXO3a in the Mitochondria, as well as increases FOXO3a Dependent Gene expression. International journal of biological sciences. 2008; 4:291–299. [PubMed: 18781224]

Knudson AG Jr. Mutation and cancer: statistical study of retinoblastoma. Proc Natl Acad Sci U S A. 1971; 68:820–823. [PubMed: 5279523]

Land H, Chen AC, Morgenstern JP, Parada LF, Weinberg RA. Behavior of myc and ras oncogenes in transformation of rat embryo fibroblasts. Mol Cell Biol. 1986; 6:1917–1925. [PubMed: 3785184]

Lombard DB, Alt FW, Cheng HL, Bunkenborg J, Streeper RS, Mostoslavsky R, Kim J, Yancopoulos G, Valenzuela D, Murphy A, et al. Mammalian Sir2 Homolog SIRT3 Regulates Global Mitochondrial Lysine Acetylation. Mol Cell Biol. 2007

Onyango P, Celic I, McCaffery JM, Boeke JD, Feinberg AP. SIRT3, a human SIR2 homologue, is an NAD-dependent deacetylase localized to mitochondria. Proc Natl Acad Sci U S A. 2002; 99:13653–13658. [PubMed: 12374852]

Parada LF, Land H, Weinberg RA, Wolf D, Rotter V. Cooperation between gene encoding p53 tumour antigen and ras in cellular transformation. Nature. 1984; 312:649–651. [PubMed: 6390217]

Rhodes DR, Kalyana-Sundaram S, Mahavisno V, Varambally R, Yu J, Briggs BB, Barrette TR, Anstet MJ, Kincead-Beal C, Kulkarni P, et al. Oncomine 3.0: genes, pathways, and networks in a collection of 18,000 cancer gene expression profiles. Neoplasia. 2007; 9:166–180. [PubMed: 17356713]

Richardson AL, Wang ZC, De Nicolo A, Lu X, Brown M, Miron A, Liao X, Iglehart JD, Livingston DM, Ganesan S. X chromosomal abnormalities in basal-like human breast cancer. Cancer cell. 2006; 9:121–132. [PubMed: 16473279]

Rogina B, Helfand SL. Sir2 mediates longevity in the fly through a pathway related to calorie restriction. Proc Natl Acad Sci U S A. 2004; 101:15998–16003. [PubMed: 15520384]

Saunders LR, Verdin E. Sirtuins: critical regulators at the rossroads between cancer and aging. Oncogene. 2007; 26:5489–5504. [PubMed: 17694089]

Schwer B, North BJ, Frye RA, Ott M, Verdin E. The human silent information regulator (Sir)2 homologue hSIRT3 is a mitochondrial nicotinamide adenine dinucleotide-dependent deacetylase. J Cell Biol. 2002; 158:647–657. [PubMed: 12186850]

Sebastian T, Malik R, Thomas S, Sage J, Johnson PF. C/EBPbeta cooperates with RB:E2F to implement Ras(V12)-induced cellular senescence. Embo J. 2005; 24:3301–3312. [PubMed: 16107878]

Serrano M, Lin AW, McCurrach ME, Beach D, Lowe SW. Oncogenic ras provokes premature cell senescence associated with accumulation of p53 and p16INK4a. Cell. 1997; 88:593–602. [PubMed: 9054499]

Sherr CJ. Principles of tumor suppression. Cell. 2004; 116:235–246. [PubMed: 14744434]

Sinclair DA. Toward a unified theory of caloric restriction and longevity regulation. Mechanisms of ageing and development. 2005; 126:987–1002. [PubMed: 15893363]

Singh KK. Mitochondria damage checkpoint, aging, and cancer. Ann N Y Acad Sci. 2006; 1067:182–190. [PubMed: 16803984]

Slane BG, Aykin-Burns N, Smith BJ, Kalen AL, Goswami PC, Domann FE, Spitz DR. Mutation of succinate dehydrogenase subunit C results in increased O2.-, oxidative stress, and genomic instability. Cancer Res. 2006; 66:7615–7620. [PubMed: 16885361]

Sotiriou C, Wirapati P, Loi S, Harris A, Fox S, Smeds J, Nordgren H, Farmer P, Praz, Spitz DR, Azzam EI, Li JJ, Gius D. Metabolic oxidation/reduction reactions and cellular responses to ionizing radiation: a unifying concept in stress response biology. Cancer Metastasis Rev. 2004; 23:311–322. [PubMed: 15197331]

Sundaresan NR, Gupta M, Kim G, Rajamohan SB, Isbatan A, Gupta MP. Sirt3 blocks the cardiac hypertrophic response by augmenting Foxo3a-dependent antioxidant defense mechanisms in mice. The Journal of clinical investigation. 2009

Tissenbaum HA, Guarente L. Increased dosage of a sir-2 gene extends lifespan in Caenorhabditis elegans. Nature. 2001; 410:227–230. [PubMed: 11242085]

Wang RH, Sengupta K, Li C, Kim HS, Cao L, Xiao C, Kim S, Xu X, Zheng Y, Chilton B, et al. Impaired DNA damage response, genome instability, and tumorigenesis in SIRT1 mutant mice. Cancer cell. 2008; 14:312–323. [PubMed: 18835033]

Warburg O. On the origin of cancer cells. Science. 1956; 123:309–314. [PubMed: 13298683]

SIGNIFICANCE

The incidence of human malignancies increases significantly with age, suggesting a mechanistic connection between aging (longevity) and carcinogenesis. One aspect of that connection is impaired mitochondrial function, which is observed in both aging cells and cancer cells as aberrant oxidative metabolism. Sirtuin family genes regulate longevity in yeast, *C. elegans*, and *D. melanogaster*, and in mammals, three of the seven sirtuin genes are localized to the mitochondria, including *SIRT3*. These observations led us to hypothesize that *SIRT3* might be a tumor suppressor that protects against carcinogenesis by maintaining mitochondrial integrity and efficient oxidative metabolism. The current work demonstrates that the loss of function of SIRT3 results in a cellular environment permissive for carcinogenesis and characterized by aberrant oxidative metabolism.

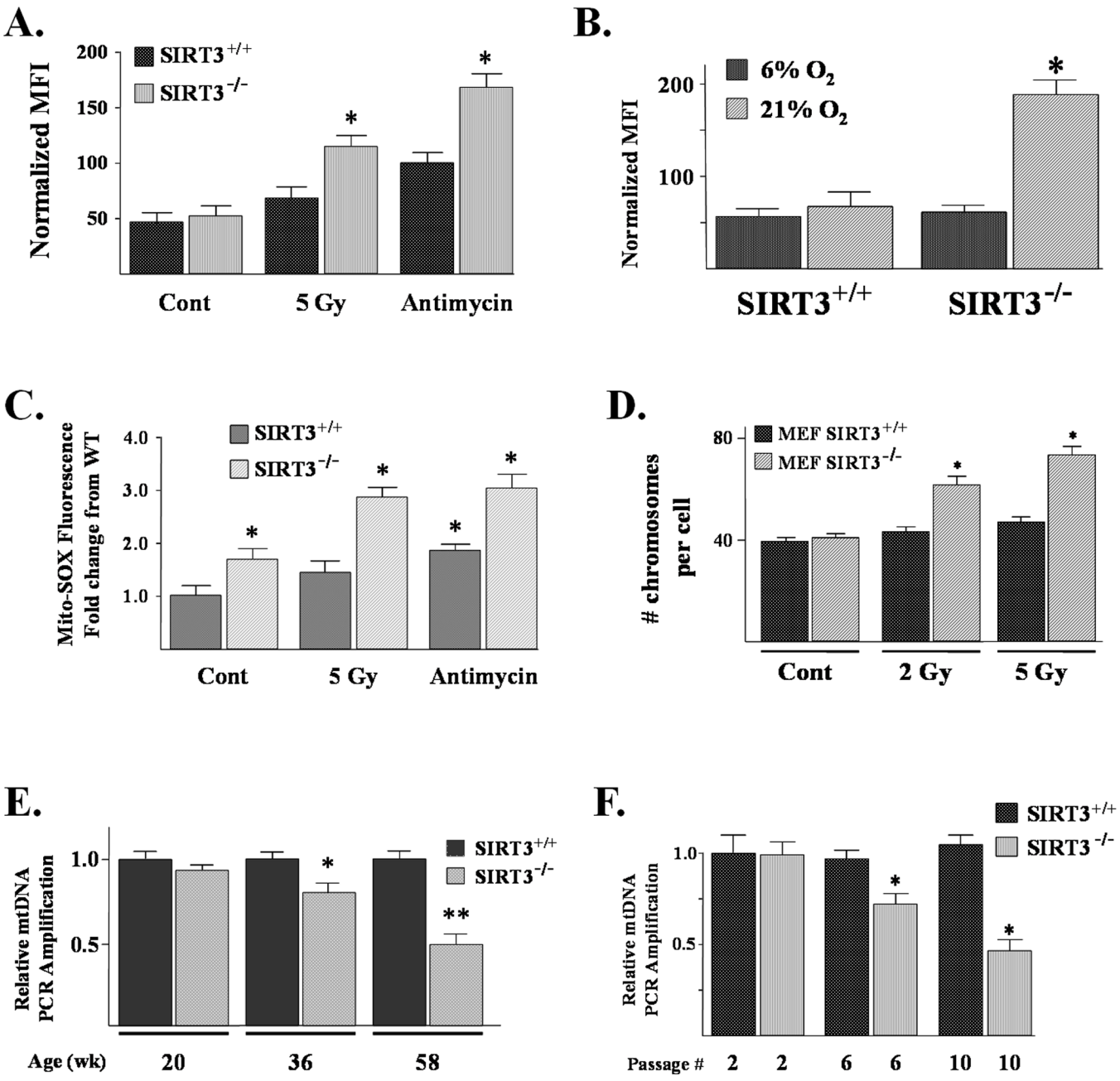

Figure 1. *SIRT3* knockout MEFs exhibit increased superoxide levels, aneuploidy in response to exogenous stress, and decreased mitochondrial integrity with increasing age

(**A**) Superoxide levels were elevated in *SIRT3* knockout cells exposed to agents that induce mitochondrial damage. $SIRT3^{+/+}$ and $SIRT3^{-/-}$ MEFs were cultured in 6% oxygen and exposed to either 5 Gy of IR or 5 μM of antimycin A for 3 hours, and superoxide levels were monitored by DHE oxidation as compared to control, untreated cells (Cont). For all DHE oxidation experiments the results were the normalized MFI for three independent replicates. (**B**) $SIRT3^{-/-}$ superoxide levels were elevated when cultured in 21% oxygen. $SIRT3^{+/+}$ and $SIRT3^{-/-}$ MEF cells were cultured at 21% O_2 for 6 hrs and superoxide levels were monitored by DHE oxidation, as compared to control cells grown at 6% O_2. (**C**) Mitochondrial superoxide levels are elevated in *SIRT3* knockout MEFs and increase

following exogenous stress. Mitochondrial superoxide levels were determined by the addition of Mito-SOX (3 μM) to the culture medium and cells were incubated for an additional 10 minutes before being trypsinized and resuspended. Fluorescence was measured via flow cytometry, and 20,000 and 40,000 cells were counted for each sample. (**D**) *SIRT3* knockout MEFs exhibited aneuploidy following exposure to IR. $SIRT3^{+/+}$ and $SIRT3^{-/-}$ MEFs were exposed to either 2 or 5 Gy. Whole-mount chromosomes were counted in a blinded fashion. Bars show the mean chromosome number per cell from 100 separate counts. (**E**) Livers from *SIRT3* knockout mice have increased mtDNA damage with age. DNA was isolated from the livers of *SIRT3* wild-type and knockout mice at 20, 36, and 58 weeks, and mtDNA primers that amplify either the 10 kb Amplicon or a 117 bp region (Supplemental Fig. S4A) were used for PCR. Primers to the genomic p-globin gene were used as a control. (**F**) *SIRT3* knockout MEFs have decreased mtDNA integrity. DNA was isolated from $SIRT3^{+/+}$ and $SIRT3^{-/-}$ MEFs at passage 2, 6, and 10, and mtDNA primers that amplify either the 10 kb Amplicon used for PCR. All the results in this figure are from at least three separate experiments. Data are presented as the average +/− SD. * indicates $P < 0.05$ by t-test. See also Figure S1.

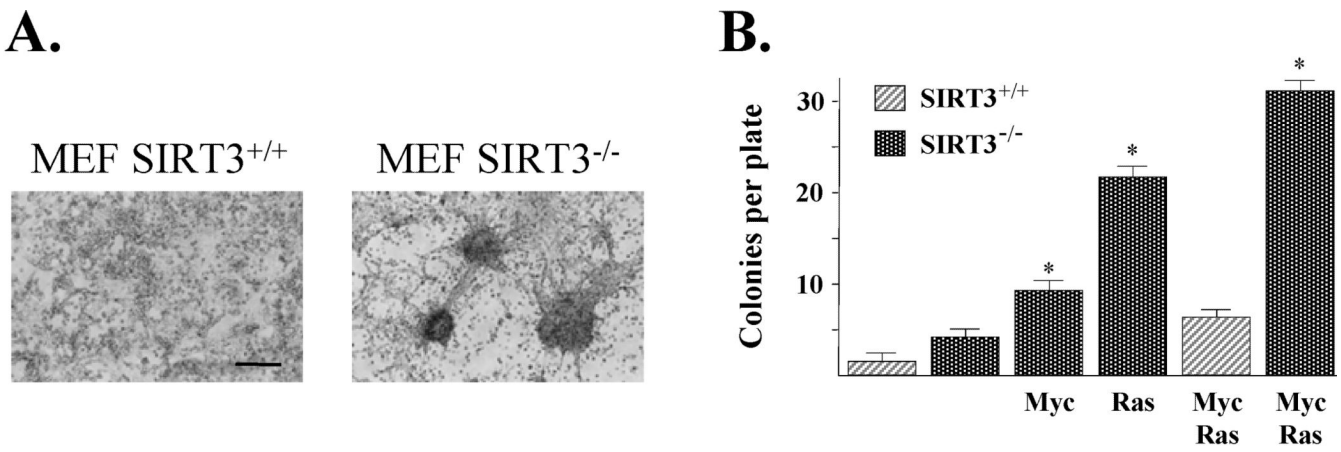

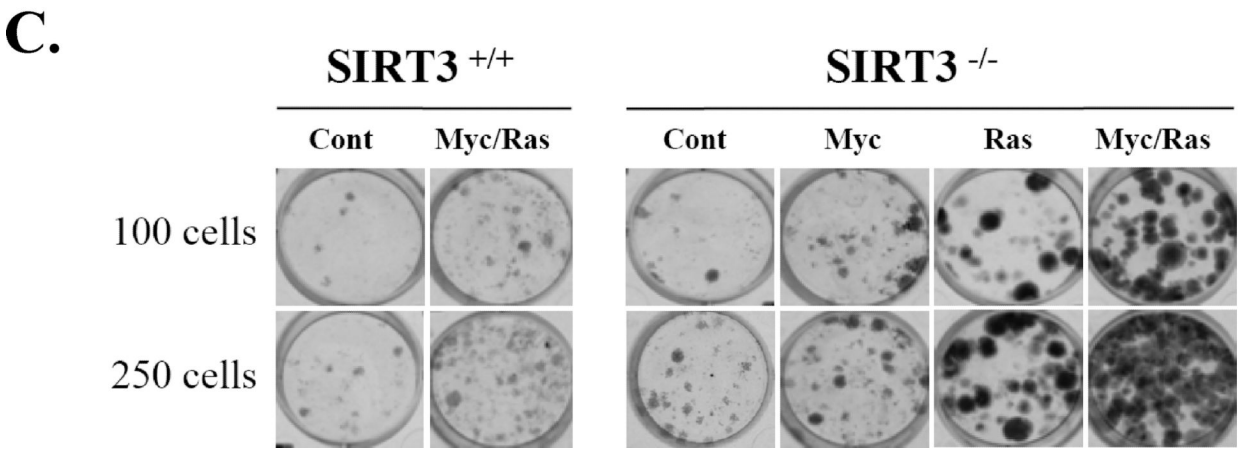

Figure 2. *SIRT3* knockout MEFs expressing a single oncogene exhibit an *in vitro* transformation-permissive phenotype

(**A**) Long-term culture (28 days) of confluent *SIRT3* knockout MEFs results in decreased contact inhibition as shown by spontaneous colony formation. $SIRT3^{+/+}$ and $SIRT3^{-/-}$ MEFs were plated at 1×10^6/100 mm dish and fed with fresh media every 3–4 days for a total of 28 days. Colonies were evident by both phase-contrast microscopy and H&E stain. (**B**) $SIRT3^{-/-}$ MEFs infected with *Myc, Ras*, or both demonstrated decreased contact inhibition. $SIRT3^{+/+}$, $SIRT3^{-/-}$, $SIRT3^{+/+}$ Myc/Ras, $SIRT3^{-/-}$ Myc, $SIRT3^{-/-}$ Ras, and $SIRT3^{-/-}$ Myc/Ras cells were plated as above and medium was replaced every 2 days for 28 days. Cells were then stained with crystal violet and counted. (**C**) *SIRT3* knockout Myc, Ras, and Myc/Ras MEFs exhibit an increased pro-proliferative growth phenotype when plated at very low densities. $SIRT3^{+/+}$, $SIRT3^{+/+}$ Myc/Ras, $SIRT3^{-/-}$, $SIRT3^{-/-}$ Myc, $SIRT3^{-/-}$ Ras, and $SIRT3^{-/-}$ Myc/Ras MEFs were plated at either 100 or 250 cells per plate (6-well plates), stained with crystal. For B–C, all results are from at least three separate experiments. Data are presented as the average +/− SD. * indicates $P < 0.01$ by t-test. Scale bar = 3 mm in (A). See also Figure S2.

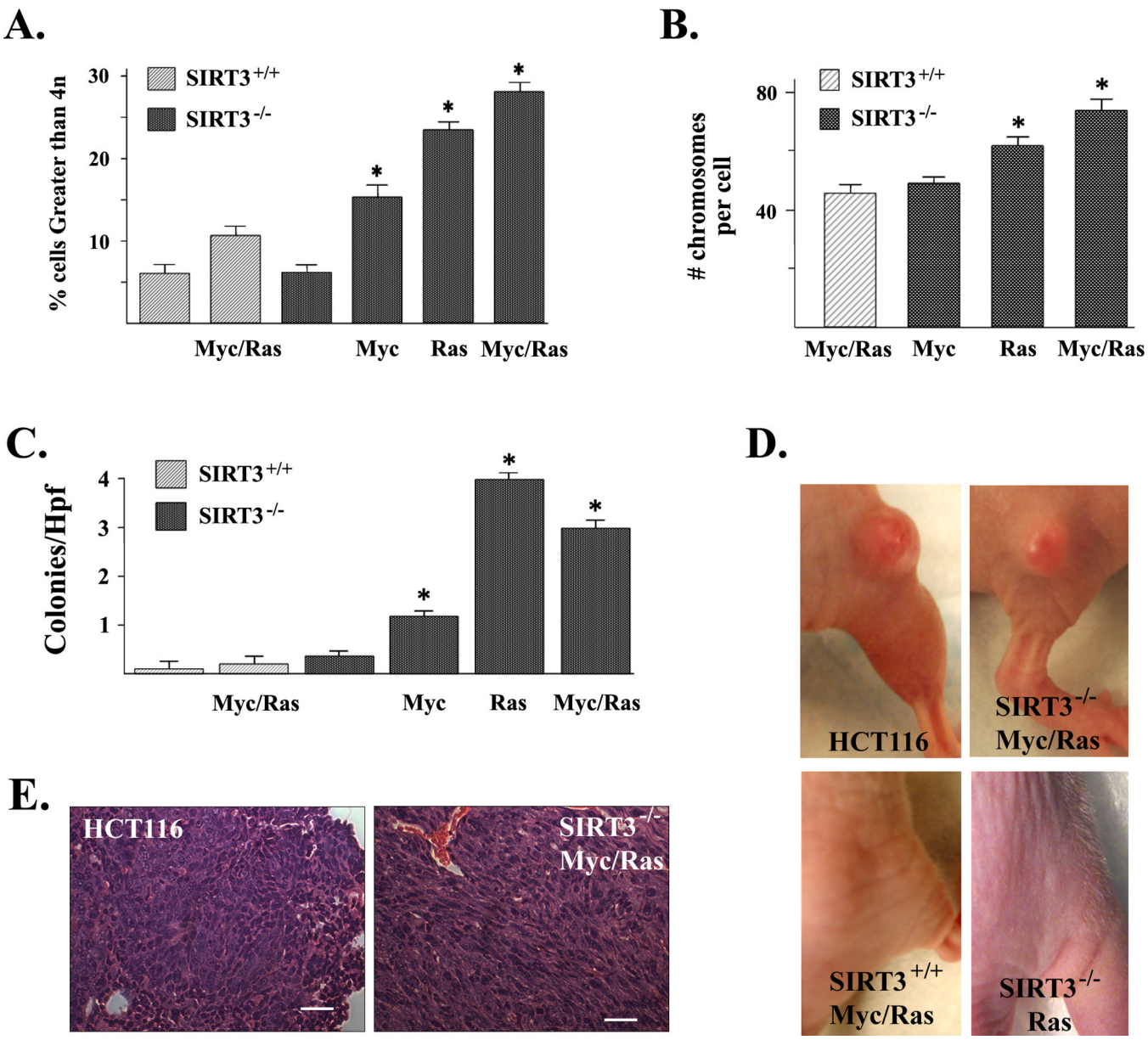

Figure 3. Loss of *SIRT3* results in an invasive and tumorigenic phenotype

(**A**) *SIRT3* knockout MEFs expressing *Myc* and/or *Ras* exhibit polyploidy. Transformed MEF cells were harvested and analyzed by FACS. The percentage of cells containing greater than 4n is shown. (**B**) SIRT3$^{-/-}$ Myc and/or Ras MEFs exhibit increased chromosomal aberrations. Whole-mount chromosomes were counted in a blinded fashion. Columns are the mean chromosome number per cell from 100 separate counts. (**C**) *SIRT3* knockout MEFs expressing *Ras* or *Myc* or both display anchorage independent growth in soft agar. SIRT3$^{+/+}$, SIRT3$^{-/-}$, SIRT3$^{+/+}$ Myc/Ras, SIRT3$^{-/-}$ Myc, SIRT3$^{-/-}$ Ras, and SIRT3$^{-/-}$ Myc/Ras cells were seeded and colonies were stained with methylene blue after 12 days and counted. (**D**) SIRT3$^{+/+}$, SIRT3$^{-/-}$, SIRT3$^{+/+}$ Myc/Ras, SIRT3$^{-/-}$ Myc, SIRT3$^{-/-}$ Myc/Ras, and SIRT3$^{-/-}$ Ras cells were implanted into both hind limbs of nude mice. Photographs of the hind limbs of nude mice injected with the cells are shown. (**E**) Histological examination of SIRT3$^{-/-}$ Myc/Ras allograft tumors stained with H&E. Results in this figure are the mean of at least three separate experiments. Error bars represent one

standard deviation about the arithmetic mean. * indicates $P < 0.05$ by t-test. Scale bar = 80 μm in (E).

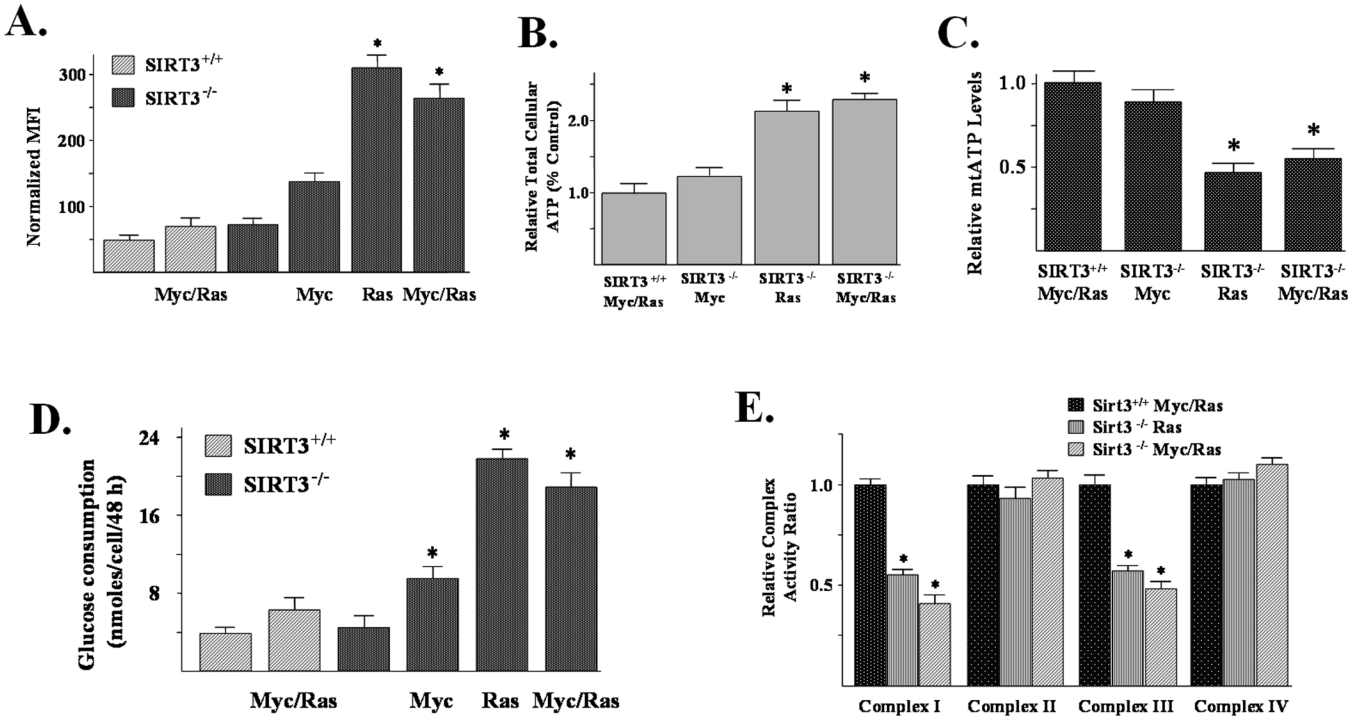

Figure 4. *SIRT3* knockout MEFs expressing *Myc* and/or *Ras* have altered biochemical and metabolic properties and exhibit decreased complex I and III activity

(**A**) Superoxide levels in *SIRT3* wild-type and knockout *Myc*- and/or *Ras*- infected MEF cells, monitored by DHE oxidation. MFI of three independent replicates was plotted. (**B**) Total cellular ATP levels in SIRT3$^{+/+}$ Myc/Ras, SIRT3$^{-/-}$ Myc, SIRT3$^{-/-}$ Ras, and SIRT3$^{-/-}$ Myc/Ras. Cells were lysed and ATP levels were measured using chemiluminescence. (**C**) Mitochondrial ATP levels are decreased in *SIRT3* knockout cells expressing either *Ras* or *Myc* and *Ras*. SIRT3$^{+/+}$ Myc/Ras, SIRT3$^{-/-}$ Myc, SIRT3$^{-/-}$ Ras, and SIRT3$^{-/-}$ Myc/Ras cells were treated with 20 mM 2DG for 4 hours and mtATP levels were measured using chemiluminescence. Data are presented as relative mtATP levels as a percentage relative to the SIRT3$^{+/+}$ Myc/Ras (Control) cells. (**D**) Analysis of glucose consumption in *SIRT3* wild-type and knockout cells infected with *Myc* and/or *Ras*. Cells were counted and medium samples were obtained at 48 hours and analyzed using an YSI glucometer. Glucose consumption was determined by subtracting glucose content at the 48-hour point from the time zero sample and dividing by the number of cells. (**E**) SIRT3$^{-/-}$ Ras and SIRT3$^{-/-}$ Myc/Ras cells exhibit decreased complex I and III activity. Oxidative phosphorylation enzyme activities were measured on total cellular protein. Complex I activity was measured as the rotenone inhibitable rate of NADH oxidation. Complex II activity was measured by the succinate induced rate of reduction of DCIP. Complex III activity was measured as the rate reduction of cytochrome c (III) when stimulated with CoQ2H2. Complex IV activity was measured as the rate of cytochrome c (II) oxidation. All enzyme complex activities are expressed relative to SIRT3$^{+/+}$ Myc/Ras. Results are from three separate experiments. Data are presented as the average +/− SD. * indicates $P < 0.05$ by t-test. See also Figure S3.

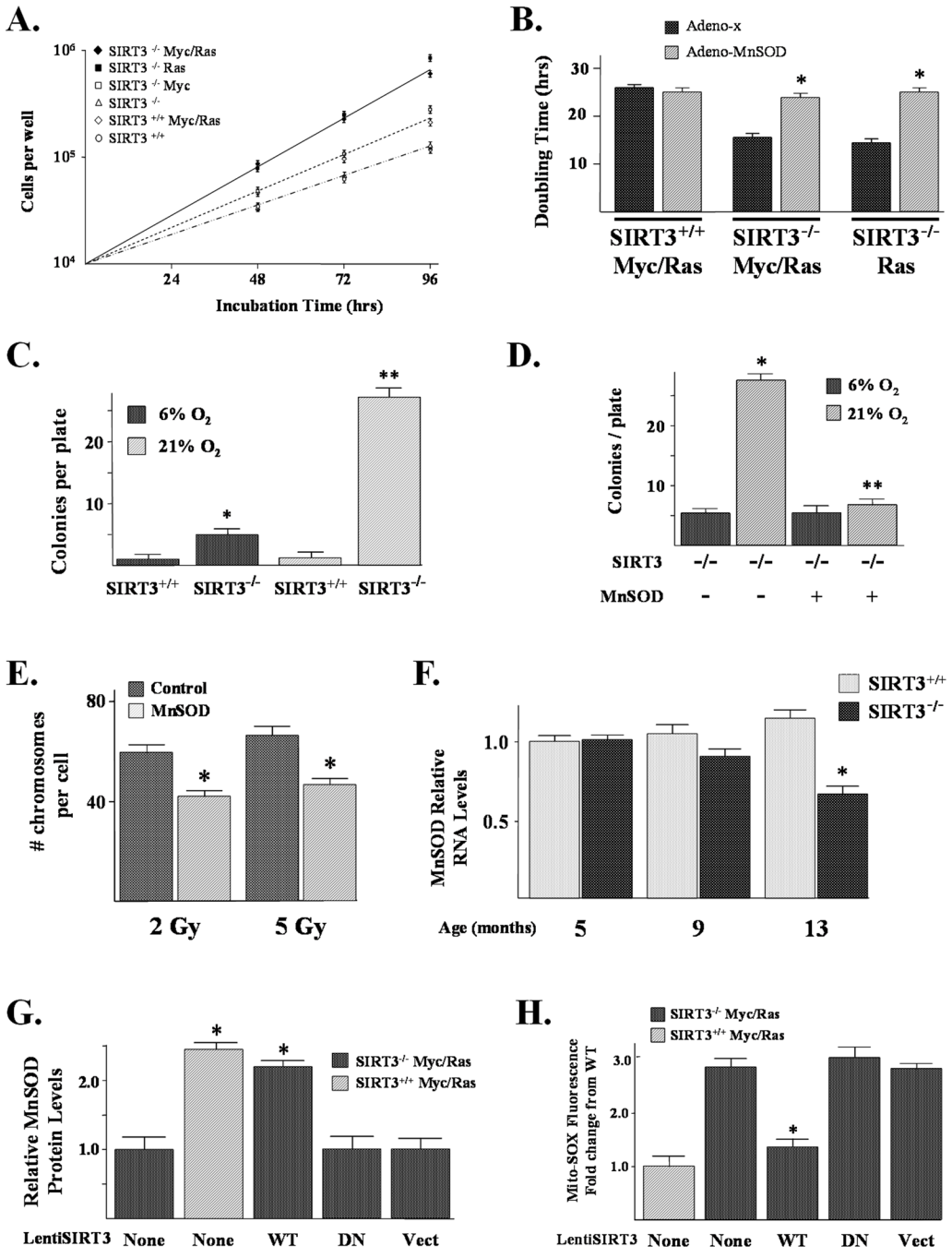

Figure 5. The transformative and growth properties of transformed *SIRT3* knockout cells are decreased by SOD

(**A**) *SIRT3* knockout cells exhibited an increased growth rate. $SIRT3^{+/+}$, $SIRT3^{-/-}$, $SIRT3^{-/-}$ Myc, $SIRT3^{-/-}$ Ras, $SIRT3^{+/+}$ Myc/Ras, and $SIRT3^{-/-}$ Myc/Ras MEFs were plated at 2×10^4 cells per plate and harvested at 2, 3, and 4 days. The number of cells per plate was plotted as a function of days to determine growth rate and doubling times. (**B**) Infection with a MnSOD-expressing adenovirus decreases the growth rate of *SIRT3* knockout cells. $SIRT3^{+/+}$ Myc/Ras, $SIRT3^{-/-}$ Myc/Ras, and $SIRT3^{-/-}$ Ras cells were infected with Adeno-MnSOD and cells were isolated at 72 and 90 hours to determine cell growth rates. (**C**) $SIRT3^{-/-}$ MEFs exhibit increased *in vitro* colony formation at 21% O_2. 1

$\times 10^6$ SIRT3$^{+/+}$ and SIRT3$^{-/-}$ MEFs were plated on a 10 cm plate and cultured at either 6% or 21% O_2. Media was replaced every 2 days and after 28 days the MEFs were subsequently stained with crystal violet and counted. (**D**) The addition of *MnSOD* reverses the increase in contact-inhibited growth in SIRT3$^{-/-}$ cells at 21% O_2. SIRT3$^{-/-}$ MEFs were plated and cultured at either 6% or 21% O_2 with infection with either 5 MOI of either a control lentivirus or a lentivirus containing *MnSOD*. Cells were subsequently stained with crystal violet and counted as above. (**E**) *MnSOD* prevents aneuploidy in *SIRT3* knockout MEFs exposed to IR. SIRT3$^{-/-}$ MEFs were infected with either a control lentivirus or lenti-MnSOD 24 hours prior to exposure to 2 or 5 Gy. Whole-mount chromosomes were counted in a blinded fashion. Bars show the mean chromosome number per cell from 100 separate counts. (**F**) *MnSOD* expression in wild-type and *SIRT3* knockout mouse livers at 5, 9, and 13 months. RNA was harvested from four age matched SIRT3$^{+/+}$ and SIRT3$^{-/-}$ mouse livers and *MnSOD* expression was determined by qRT-PCR using *MnSOD* and β-*actin* Taqman probes (ABI). (**G**) Infection of lenti-SIRT3-wt but not lenti-SIRT3-dn (deacetylation null mutant) increases MnSOD protein levels in SIRT3$^{-/-}$ Myc/Ras transformed MEFs. SIRT3$^{-/-}$ Myc/Ras cells were infected with virus, and 48 hours later cells were harvested and extracts were isolated and 20 μg of protein were separated by SDS-PAGE, transferred onto nitrocellulose, and immunoblotted using an anti-MnSOD antibody (Cell Signaling Technology, Inc). (**H**) Infection of lenti-SIRT3-wt but not lenti-SIRT3-dn in SIRT3$^{-/-}$ Myc/Ras transformed MEFs reverses the increase in mitochondrial superoxide levels. Mitochondrial superoxide levels were determined by the addition of Mito-SOX (3 μM) to the culture medium and cells were incubated for an additional 10 minutes before being trypsinized and resuspended. Fluorescence was measured via flow cytometry, and 20,000 and 40,000 cells were counted for each sample. Results are from at least three separate experiments. Data are presented as the average +/− SD. * indicates $P < 0.05$ and ** indicates $P < 0.01$ by t-test. See also Figure S4.

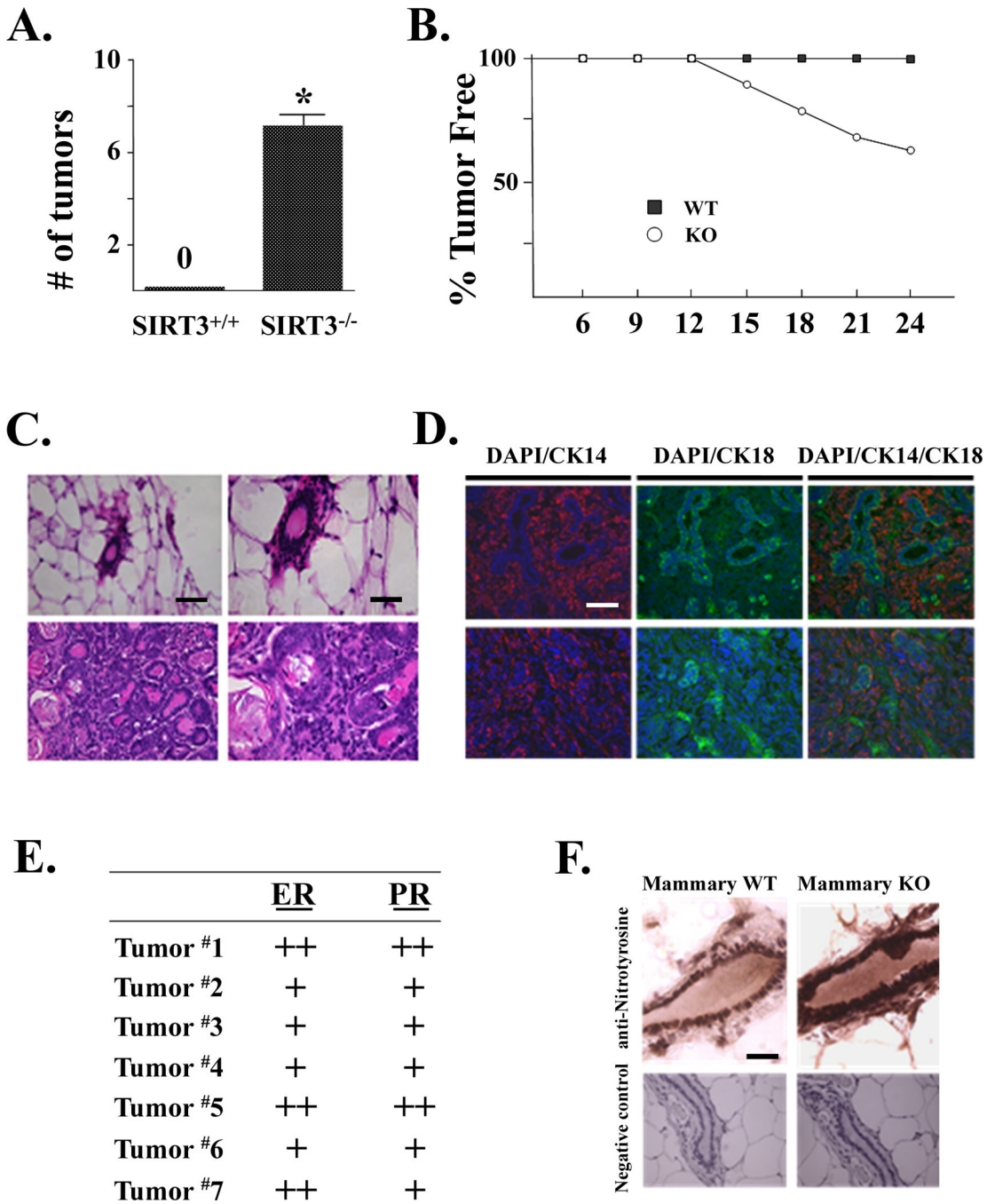

Figure 6. *SIRT3* is a mitochondrial localized murine tumor suppressor

(**A**) *SIRT3* knockout mice develop mammary tumors. The total number of mammary tumors at 24 months in *SIRT3* wild-type and knockout mice is shown. Data are presented as the average +/− SD. * indicates $P < 0.05$ by t-test. (**B**) Plot of the number of tumor-free $SIRT3^{-/-}$ ($n = 10 \times 2$) and wild-type mice ($n = 12 \times 2$) over 24 months. (**C**) Representative H & E slides from mammary tissue from a $SIRT3^{+/+}$ and a $SIRT3^{-/-}$ mouse that developed a mammary tumor. (**D**) IHC staining of $SIRT3^{-/-}$ murine mammary tumors with DAPI/CK14 (left panel), DAPI/CK18 (middle panel), and merged (right panel). (**E**) IHC staining for ER and PR status was performed on paraffin sections from the seven $SIRT3^{-/-}$ mice that

developed mammary tumors. ER/PR levels were characterized as absent (−), intermediate (+), or strongly present throughout the sample (++). (**F**) *SIRT3* knockout mice mammary ductal cells exhibit increased anti-nitrotyrosine IHC staining. Mammary tissue from four $SIRT3^{+/+}$ and $SIRT3^{-/-}$ mice at age 12 months was stained with an anti-nitrotyrosine antibody (StressMarq Biosciences Inc.). A representative micrograph is shown. Scale bar = 160 μm in (C, left panel), 80 μm in (C, right panel) and (F), and 40 μm in (D). See also Figure S5.

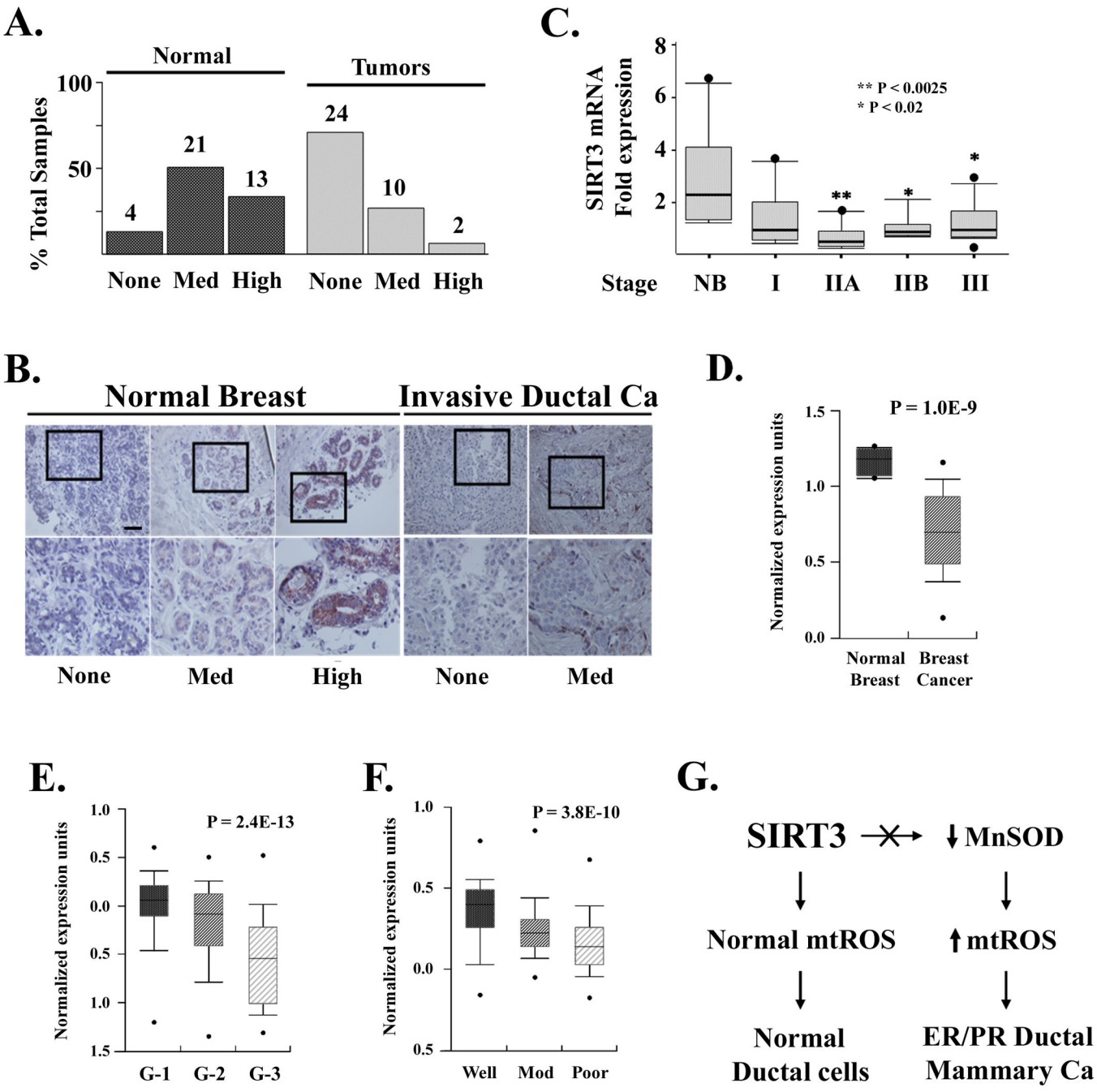

Figure 7. *SIRT3* is a potential human tumor suppressor

(**A**) SIRT3 protein levels are decreased in human breast tumors; 38 normal and 36 breast cancer (US Biomax, Inc) samples were measured by IHC on a tissue array. Tissue arrays were stained with a human SIRT3 antibody (Cell Signaling Technology, Inc) and slides were read by two independent researchers. Levels of SIRT3 staining were classified as absent, medium, or high. (**B**) IHC images from breast tumor and normal samples demonstrating SIRT3 staining. The boxed regions (enlarged in the bottom row) show SIRT3 in normal epithelium (left six images) and breast tumors (right four images). (**C**) *SIRT3* expression in RNA samples from normal breast (NB) and Stage I, IIA, IIB, and III breast malignancies (TissueScan Breast Cancer Panel 1 Origene). *SIRT3* expression was

determined by qRT-PCR using *SIRT3* and β-*actin* Taqman probes (ABI). (**D-F**) *SIRT3* expression is decreased in human breast cancer and as a function of pathological classification. The Oncomine cancer microarray database (http://www.oncomine.org) was used to determine *SIRT3* expression in (**D**) normal versus breast cancers (Richardson et al., 2006), as a function of (**E**) Elston (G-1, G-2, or G-3) Grade (Ivshina et al., 2006), or (**F**) pathological (well, moderately, or poorly differentiated) differentiation (Sotiriou et al., 2006). The y-axis represents normalized expression units. Shaded boxes represent the interquartile range; whiskers represent the 10th-90th percentile range; bars represent the median. (**G**) Schema for the development of increased mtROS and ER/PR positive mammary tumors in ductal cells lacking *SIRT3*. Scale bar = 80 μm in (B). See also Figure S6.

TABLE 1

Immortalization of SIRT3$^{-/-}$ MEFs only requires a single oncogene

MEFs	Control	Myc	Ras	Myc/Ras
SIRT3$^{+/+}$	None	None	None	Immort
SIRT3$^{-/-}$	None	Immort	Immort	Immort
SIRT3$^{-/-}$ + Lenti-MnSOD	None	None	None	Immort
SIRT3^{wt}-SIRT3$^{-/-}$	None	None	None	Immort
SIRT3^{dn}-SIRT3$^{-/-}$	None	Immort	Immort	Immort

None, no MEF immortalization.

Immort, immortalization.

Lenti-MnSOD, lentiviral-MnSOD 10 MOI.

Immortalization experiments were done in triplicate.